京都大学防災研究所年報 第 53 号 B 平成 22 年 6 月
Annuals of Disas. Prev. Res. Inst., Kyoto Univ., No. 53 B, 2010

Experimental and FE Analysis of Seismic Soil-Pile-Superstructure Interaction in Sand

Mahmoud N. HUSSIEN*, Tetsuo TOBITA and Susumu IAI

* Graduate School of Engineering, Kyoto University

Synopsis

Seismic response of end bearing piles supporting simple structures founded on a homogeneous dense sand layer over rigid rock is studied using a geotechnical centrifuge at DPRI-KU. Experiments are carried out under the centrifugal acceleration of 40G. The pile foundation is excited by a shaking table at the pile tip with and without the superstructure using sinusoidal waves with different amplitudes and different frequencies to investigate the inertial effect of the superstructure on the pile response. Nonlinear dynamic analyses using the 2-D finite element (FE) method are compared to the recorded responses during shaking in the centrifuge. The soil-pile interaction in 3-D is idealized in 2-D type using soil-pile interaction springs with hysteretic nonlinear load displacement relationships. Computed time histories of pile head acceleration and displacement, except for bending moment, were consistent with those obtained from experiments. Numerical analysis tends to under-estimate the maximum value of the bending moment, because of the empirical procedure for the setting of soil-pile interaction springs.

Keywords: Pile, finite element, centrifuge, dynamic bending moment

1. Introduction

In highly seismic areas such as Japan, seismic soil-pile-superstructure interaction (SSPSI) problems have received considerable attention in recent years. Although, the shortage of data from actual earthquakes limits the further progress in this research field, it motivates researchers to perform centrifuge and shaking table model tests. The use of centrifuge tests offers the advantages of modeling complex systems under controlled condition. Also, numerical models procedures can be calibrated and improved or modified for phenomena that may not have been adequately accounted for in a model (Rayhani and El Naggar, 2008). Several numerical and analytical methods have been proposed for the analysis of SSPSI based on simplified interactions models such as the beam on dynamic Winkler Foundation approach (Kagawa and Kraft, 1980; Allotey and El Naggar, 2008), as well as those based on more rigorous FEM (Cai et al., 1996: Rovithis et al., 2009), or BEM (Padrón et al., 2007), formulations. These methods utilize either simplified two-step methods that uncouple the superstructure and foundation portions (Gazetas 1984; Beltrami et al., 2005) or a fully coupled SSPSI system in a single step (Kaynia and Mahzooni 1996; Mylonakis et al., 1997). Although the former provides insights as to the distinct role of inertial and kinematic interaction, the latter gives a direct and more convenient estimation of the complete system response (Rovithis et al., 2009). The coupled 3-D FE approach is most representative of the SSPSI system, but is computationally intensive and time consuming. Ozutsumi et al., (2003) proposed a method to

idealize the soil-pile interaction in 3-D into the 2-D type using soil-pile interaction springs that connect pile elements to 2-D meshes of a soil profile.

This article presents experimental results and analysis of centrifuge tests that were conducted to investigate the SSPSI then the experimental results are used to check the applicability of the 2-D FE program **FLIP** incropating the interaction spring proposed by Ozutsumi et al., (2003). A schematic view of the system under investigation is shown in Fig. 1. Details of centrifuge models with test results and the FE models are briefly summarized. Then the results of the FE and centrifuge models are compared in terms of time histories of soil and structural responses. The test results of centrifuge are presented in terms of prototype unless otherwise stated.

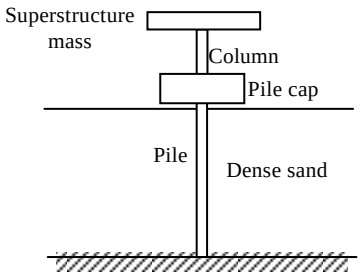

Fig.1 A schematic view of the system under investigation

2. Experimental setups and procedures

The model tests were performed using the geotechnical centrifuge at the Disaster Prevention Research Institute, Kyoto University (DPRI-KU). The centrifuge has a radius of 2.5 m and consists of a balanced arm with dual swing platforms. The maximum capacity is 24 g-tons with a maximum centrifugal acceleration of 200 g. A shake table driven unidirectionally by a servo hydraulic actuator is attached to a platform and it is controlled through a personal computer (PC) on the centrifuge arm. All the equipment necessary for shake table control is put together on the arm. The PC is accessible during flight from a PC in the control room through wireless LAN and "Remote Desktop Environment". The shake table has the capacity of 15 kN, 10g and ± 2.5 mm in maximum force, acceleration and displacement, respectively (Tobita et al., 2006). All tests were carried out in the centrifugal acceleration field of 40g using a rigid soil container with inner dimension of 0.45 m (L) × 0.15 m (W) × 0.29 m (H).

The model ground in this study was made of Silica sand No. 7 having the physical and mechanical properties shown in Table 1 and the particle size distribution curve shown in Fig. 2. A dry sand deposit was prepared by air pluvation. After fixing the pile in a bottom plate in the soil container base, silica sand was rained in 1 g field using a hopper fixed at the specified height until the sand deposit formed 11.6 m thick deposit (290 mm in model scale). The sand deposit was then consolidated in 40 g centrifugal acceleration field for 5 min. By measuring the heights of the ground surface after the consolidation, relative density was obtained as 85%. The soil was instrumented with accelerometers at different depths.

Table 1 Physical properties of Silica sand No. 7

e_{max}	e_{min}	D_{50}(mm)	Uc	Gs
1.19	0.710	0.13	1.875	2.66

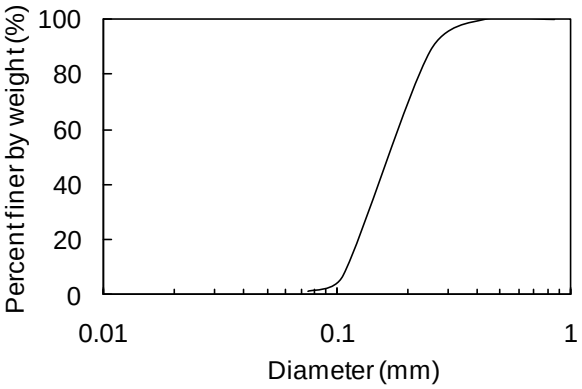

Fig. 2 Particle size distribution curve for Silica sand No.7

The pile was placed in the model before the soil was pluviated, attempting to simulate a pile installed with minimal disturbance to the surrounding soil, as may be the case when a pile inserted into a pre-augered hole. Seven strain gauges were placed at different locations along the pile to measure bending moments. The single pile was supporting a simple structure consisted of pile cap, column, and superstructure mass as shown in

Fig. 1. The pile cap and the superstructure mass were instrumented with LDTs and accelerometers to measure their displacements and accelerations. Material properties of model pile, pile cap, column, and superstructure mass used in this study are shown in Table 2, Table 3, Table 4, and Table 5 respectively. For the pile cap and the superstructure mass, the centrifuge scaling relations were applied based on mass and stiffness.

Four sinusoidal waves as input base accelerations with different amplitudes and different frequencies as shown in Table 6 were applied in series to the system without the superstructure mass. Then the superstructure mass was added and the three input base accelerations were applied to the system with the same previous manner.

Table 2 Properties of pile modeling

	Steel tube		
	Model	Prototype	Units
Length	0.29	11.6	m
Outer diameter	10	400	mm
Wall thickness	0.75	30	mm
Young's modulus	206	206	GPa
Moment of inertia	2.35×10^{2}	6.00×10^{8}	mm^4
Bending stiffness	48.41	1.24×10^{8}	$MN\text{-}mm^2$

Table 3 Properties of pile cap modeling

	Model	Prototype	Units
Mass	0.3792	24231	kg
Moment of inertia	9.0×10^{4}	2.33×10^{11}	mm^4
Bending stiffness	1.85×10^{4}	4.75×10^{10}	$MN\text{-}mm^2$

Table 4 Properties of column modeling

	Steel tube		
	Model	Prototype	Units
Length	0.075	3.0	m
Outer diameter	10	400	mm
Wall thickness	0.75	30	mm
Young's modulus	206	206	GPa
Moment of inertia	2.35×10^{2}	6.00×10^{8}	mm^4
Bending stiffness	48.41	1.24×10^{8}	$MN\text{-}mm^2$

Table 5 Properties of superstructure mass

	Model	Prototype	Units
Mass	0.297	19008	kg
Moment of inertia	1.41×10^{4}	3.61×10^{10}	mm^4
Bending stiffness	2.90×10^{3}	7.42×10^{9}	$MN\text{-}mm^2$

Table 6 Input base motions

Base acceleration	Max amplitude (g)	Frequency (Hz)
1	0.005	0.1
2	0.084	0.5
3	0.317	1.0
4	0.136	2.0

3. Test results and discussion

Fig. 3 shows the time histories of the pile cap displacements for all studied cases: the solid and broken lines correspond to the cap displacements with and without superstructure, respectively. It is

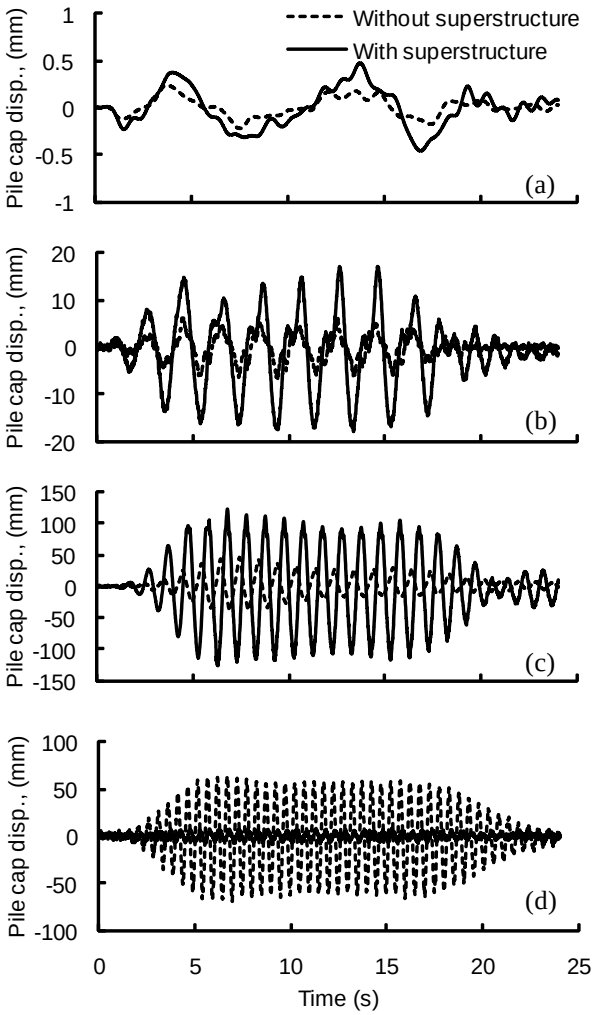

Fig.3 Time histories of pile cap displacement; 0.1 Hz (a), 0.5 Hz (b), 1.0 Hz (c) and 2.0 Hz (d)

worth to note that the effect of the inclusion of the superstructure on the pile cap displacement is not the same for all tested cases but it is frequency dependent. For the first three cases (0.1, 0.5, and 1.0 Hz), the effect of the superstructure is to increase the pile cap displacement. This effect is reversed when the frequency of the input motion is increased to 2.0 Hz.

Fig. 4 shows the maximum amplitudes of pile cap displacement versus the frequency of input motions. The variation of pile cap displacement amplification relative to ground surface (free field) displacement (U_{cap} /Ug) is also shown in Fig.5. From These two figures, the following trends can be noted:

1. The fundamental frequency of the system with the superstructure (approximately about 1.0 Hz) is smaller than that of the system without the superstructure (higher than the range of the studied cases). These values are consistent with the preliminary estimation (modal analysis) of the fundamental frequencies of the systems with and without the superstructure. Research is still on going and therefore experimental cases of input motions with higher frequencies will be conducted later to confirm this observation.
2. At low frequencies, the pile cap displacements of both cases with and without the superstructure is negligable compared to the free field displacement due to the high rigidity of the pile that constrains the pile movement relative to the soil movement especially at low frequencies as shown in Fig. 5. This means that the pile response at low frequencies is controled by its bending rigidity rather than kinematic (from soil) or inertial (from structure) effects.
3. The amplification of the pile cap displacement (with the superstructure) initates at low frequency (about 0.5 Hz) compared to the corresponding pile cap displacement (without the superstruture) that intiates from a frequency close to 0.8 Hz as shown in Fig. 5. This difference between frequencies is due to the inertial effect, comes from the superstructure mass, and it tends to increase the pile cap

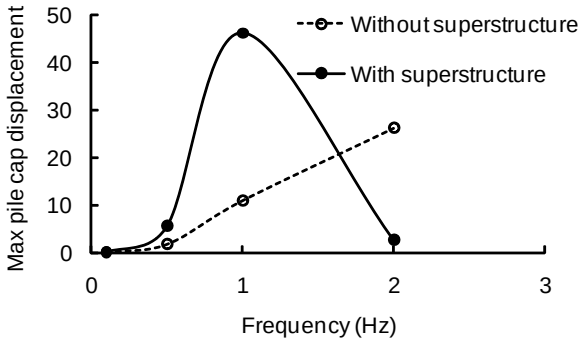

Fig.4 Maximum pile cap displacement variation with frequency

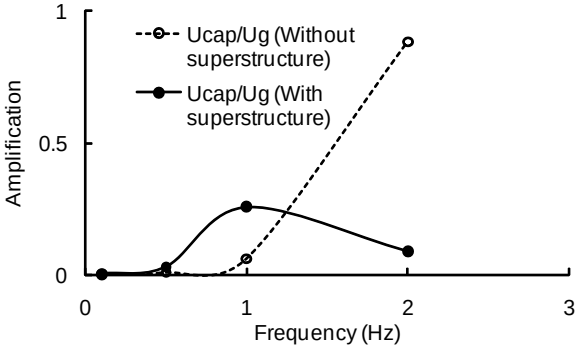

Fig.5 Amplification ratios of pile cap displacement relative to free field displacement

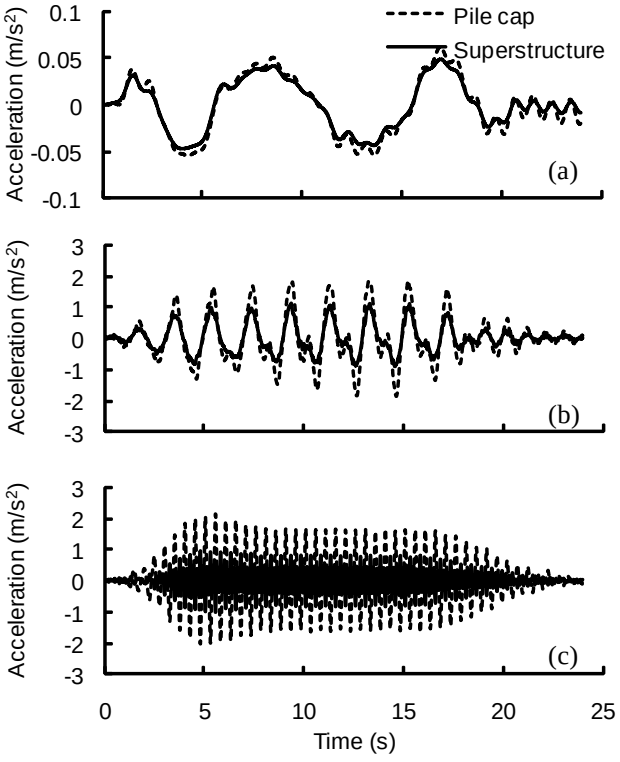

Fig.6 Pile cap and superstructure accelerations time histories; 0.1 Hz (a), 0.5 Hz (b), and 2.0 Hz (c)

displacement relative to the free field displacement up to 1.0 Hz input motion (equal to the fundmental frequency of the system). In this range, its obsarved that the pile cap and superstructure mass accelerations are in phase. After this frequency (1.0 Hz), the pile cap and superstructure mass accelerations are out of phase as shown in Fig. 6 thus the superstructure mass tends to decrease the pile cap displacement.

Fig. 7 illustrates the inertial effect of the superstructure on the peak bending moment profile, calculated as extreams bending moments at different depthes along the pile for 0.5, 1.0, and 2.0 Hz cases. The figure declares that the effect of the superstructure on the bending moment profile is simillar to its effect on the pile cap displacement.

4. Numerical simulation

The 2-D FE program FLIP (Finite element analysis program for LIquefaction Process) (Iai et al. 1992) is employed in this study. Soil is modeled as having the multi-shear mechanism. Parameters for sand used in the FE analysis were determined referring to the results of laboratory tests on Silica sand No. 7 as shown in Table 7. The bulk modulus of the soil skeleton K was determined assuming a Poisson's ratio υ of 0.33. The pile and the column are modeled with Bilinear one-dimensional beam elements. Table 8 defines the model parameters of pile and column elements. Linear plane elements with two degrees of freedom per node were used to model the pile cap and the superstructure mass. The soil-pile interaction in 3-D is idealized in 2-D type using soil-pile interaction springs with hysteretic nonlinear load displacement relationships. While the conventional spring elements used in the analysis of soil-pile interactions are embedded in the same plane of the 2-D FE analysis domain, the soil-pile interaction spring used in this study is a spring that connects a free pile to a 2-D cross section of soil (details of soil-pile spring can be found in Ozutsumi et al. (2003).

5. Comparison of calculated and recorded responses

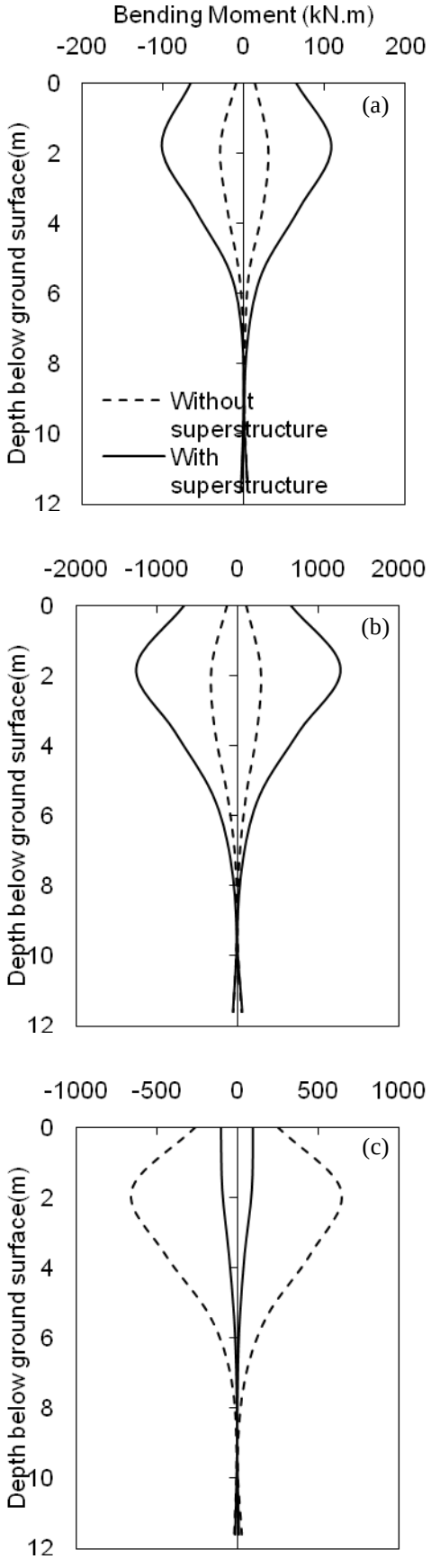

Fig. 7 Peak bending moment profile: 0.5 Hz (a), 1.0 Hz (b) and 2.0 Hz

Table 7 Model parameters for soil elements.

Density, ρ (t/m^3)	G_{ma} (kPa)	υ	σ'_{ma} (kPa)	φ_f (deg)	H_{max}
1.5	5.1×10^4	0.33	57.11	38	0.20

Table 8 Model parameters for pile and column elements.

Gs (kPa)	υ	ρ (t/m^3)	Initial flexural rigidity (kPa)	Flexural rigidity after yield (kPa)
7.75×10^7	0.29	7.9	3.64×10^5	2.47×10^5

Recorded and calculated responses of soil and pile cap for input motion of 0.5 Hz without the superstructure mass are compared in Fig. 8. The computed time histories of ground acceleration, pile cap aceleration, and pile cap displacement are consistent with the recorded ones in terms of their amplitudes and phases. Thus the FE analysis reproduced soil and pile cap responces reasonably well.

Recorded and calculated responses of soil, pile cap, and superstructure mass for the same input motion after adding the superstructure mass are compared in Fig. 9. The general trend of ground acceleration, pile cap aceleration, and pile cap displacement records was satisfactorily predicted in terms of their amplitudes and phases. The computed time history of superstructure acceleration is also consistent with the recorded one.

Figure 10 plots the peak bending moment profiles, calculated as extreams bending-moments at different depthes along the pile for input motions of 1.0 Hz and for both cases with and without the superstructure mass. This figure compares the depths where the maximum moments were measured and computed. The difference between the measured and computed depths of the maximum

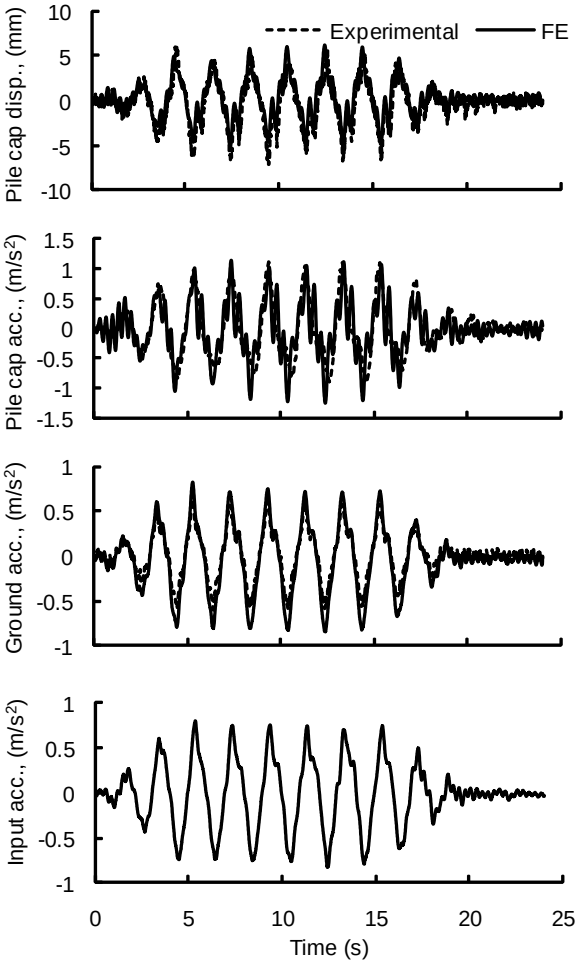

Fig. 8 Comparison of recorded and calculated ground and pile cap responses, without the superstructure, 0.5 Hz

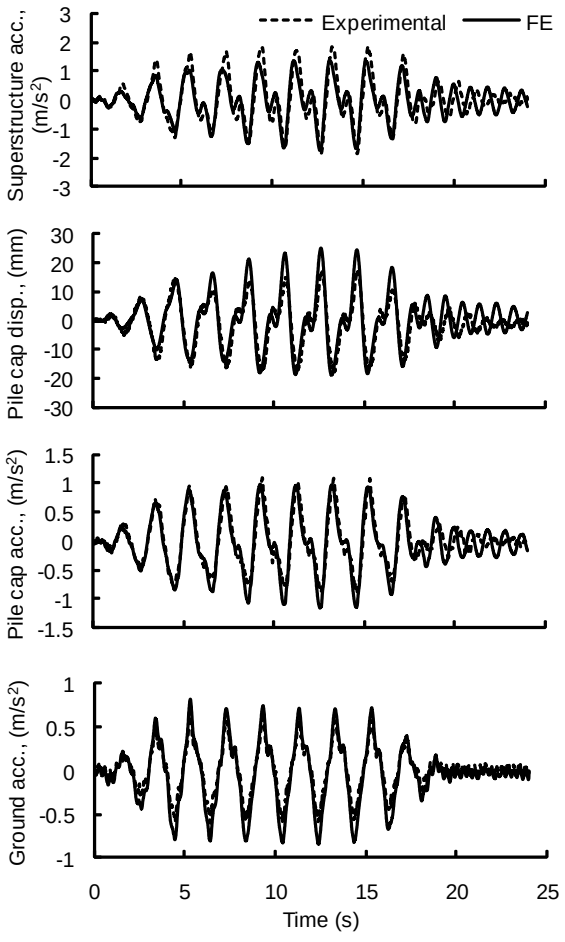

Fig. 9 Comparison of recorded and calculated ground, pile cap and superstructure responses, 0.5 Hz

bending moment was about 1.5 m. The computed depths where the bending moment returned to zero were consistent with the measured ones. The difference between the measured and computed depths was within 1.0 m.. For the system without the superstructure mass, the computed bending moment profile agreed well with the measured one. The FE is also successful at predicting the increase of peak bending moment profile after adding the superstructure mass but the computed increase of bending moment differed from the recorded one. Numerical analysis tends to under-estimate the maximum value of the bending moment and this may be due to the empirical procedure for the setting of soil-pile interaction springs.

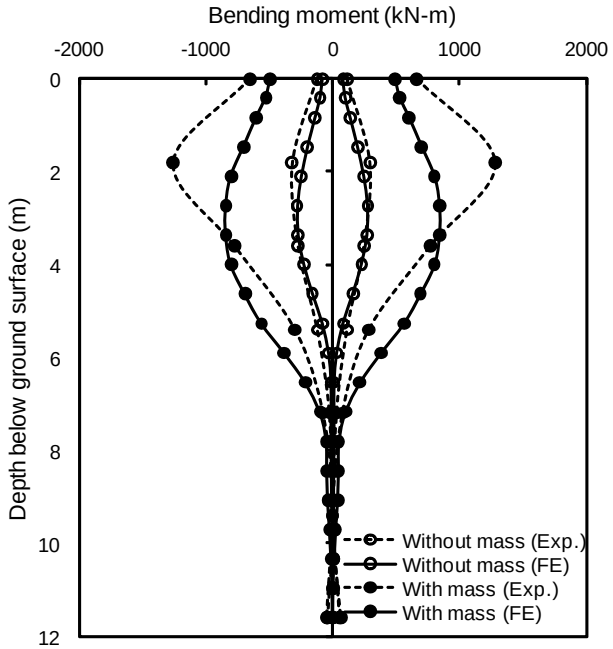

Fig. 10 Comparison of recorded and calculated peak bending moment profile, 1.0 Hz

6. Conclusions

To study the Seismic response of end bearing piles supporting simple structures, centrifuge experiments are conducted. Experimental results show that the inertial effect of the superstructure on the pile response is frequency dependent and the pile response at low frequencies is controled basicaly by its bending rigidity rather than kinematic (from soil) or inertial (from structure) effects. With the increase of the input motion frequency, the inertial effect of the superstructure on pile cap displacement strates to appear and the pile cap displacemnt reaches its maximum value relative to the free field displacement when the frequency of the input motion becomes equal to the fundamental frequency of the system, then the relative displacement of the cap gradually decrease because of the reversion of the inertial force direction.

Numerical analysis based on the effective stress analysis, FLIP, properly simulated ground surface acceleration, pile cap acceleration, pile cap displacement, and superstructure acceleration with a reasonable degree of accuracy. However, numerical analysis tends to under-estimate the maximum value of the bending moment, because of the empirical/internal procedure for the setting of soil-pile interaction springs.

References

Allotey, N. and El Naggar, M.H. (2008): Generalized dynamic Winkler model for nonlinear soil-structure interaction analysis, Canadian Geotechnical Journal, 45(4), pp. 560-573.

Beltrami, C., Lai, C.G. and Pecker, A. (2005): A kinematic interaction model for large diameter shaft foundation: An application to seismic demand assessment of a bridge subject to coupled swaying-rocking excitation. Journal of Earthquake Engineering, 9(2), pp. 355–394.

Cai, Y., Gould, P. and Desai, C. (1995): Numerical implementation of a 3-D nonlinear seismic S-P-S-I methodology, in Seismic Analysis and Design for Soil-Pile-Structure Interactions, Geotechnical Special Publication, 70, ASCE, pp. 96-110.

Gazetas, G. (1984): Seismic response of end bearing single piles. Soil Dynamics and Earthquake Engineering, 3(2), pp. 82–93.

Iai, S., Matsunaga, Y., Kameoka, T., Strain space plasticity model for cyclic mobility. Soils and Foundations, 32(2), 1–15, 1992.

Kagawa, T. and Kraft, L. (1980): Seismic P-Y responses of flexible piles, Journal of Geotechnical Engineering, ASCE, 106(8), pp. 899-918.

Kaynia, A. M. and Mahzooni, S. (1996): Forces in

pile foundations under seismic loading. Journal of Engineering Mechanics, 122(1), pp. 46–53.

Mylonakis, G., Nikolaou, A. and Gazetas, G. (1997): Soil-pile-bridge seismic interaction: kinematic and inertial effects. Part I: Soft soil. Earthquake Engineering and Structural Dynamics, 26, 337–359.

Ozutsumi, O., Tamari, Y., Oka, Y., Ichii, K., Iai, S. and Umeki, Y. (2003): Modeling of soil–pile interaction subjected to soil liquefaction in plane strain analysis, Proc. of the 38th Japan, National Conference on Geotechnical Engineering, Akita, pp. 1899–1900.

Padrón, J.A., Aznárez, J.J. and Maeso, O. (2007): BEM–FEM coupling model for the dynamic analysis of piles and pile groups, Engineering Analysis with Boundary Elements, 31(6), pp. 473-484.

Rayhani, M.H.T. and El Naggar, M.H. (2008): Seismic response of sands in centrifuge tests, Canadian Geotechnical Journal 45(4), pp. 470-483.

Rovithis, E.N., Pitilakis, K.D. and Mylonakis, G.E. (2009): Seismic analysis of coupled soil-pile-structure systems leading to the definition of a pseudo-natural SSI frequency, Soil Dynamics and Earthquake Engineering, 29(6), pp. 1005-1015.

Tobita, T., Iai, S., Sugaya, M. and Kaneko, H. (2006): Soil–pile interaction in horizontal plane: Seismic performance and simulation of pile foundations in liquefied and laterally spreading ground, Geotechnical Special Publication, ASCE, 145, pp. 294–305

砂地盤における杭－地盤－上部工の動的相互作用問題に関する実験と FEM 解析

Mahmoud N. HUSSIEN*・飛田哲男・井合進

*京都大学大学院 工学研究科

要　旨

40G場の遠心模型実験により，均一で密な砂地盤で下端支持杭を持つ2自由度構造物の動的応答について調べる。上部工の慣性力が杭基礎に与える影響を考察するため上部工の有無，入力正弦波の振幅と振動数を変化させて実験を行う。また，実験結果を2次元非線形動的有限要素解析結果と比較する。ただし，本質的に3次元の問題である杭－地盤の動的相互作用は，応力履歴を考慮できる地盤－杭相互作用ばねを導入し2次元でモデル化するものとする。加速度および変位時刻歴については実験と解析とで良い一致を示したが，曲げモーメントについては今後の検討が必要である。

キーワード：杭，有限要素法，遠心模型実験，曲げモーメント